JOURNAL OF AIRCRAFT
Vol. 35, No. 6, November–December 1998

Wake Forces Implied in the Theodorsen and Goldstein Theories of Propellers

Herbert S. Ribner*
University of Toronto, Downsview, Ontario M3H 5T6, Canada
and
NASA Langley Research Center, Hampton, Virginia 23681-0001

This study examines wake edge forces and normal forces implied, but overlooked, respectively, in the Theodorsen and Goldstein theories of the optimum efficiency of propellers. It is argued that the postulated trailing vortex sheets must coincide with real rigid surfaces to support forces exerted by the fluid. In the rigidized Theodorsen model, edge suction forces are tilted backward and circumferentially in the region of contraction. These are implicitly included in the predictions of propeller thrust and torque. The corrections are estimated herein. The resulting change in efficiency, a gain, is normally less than 1%, but can reach over 2% in extreme examples. In the rigidized Goldstein model, the wake does not contract, but the streamlines do. The crossflow component, acting on the bound trailing vortices, generates lift; hence, thrust and torque components. These corrections to the Goldstein-based predictions (using Theodorsen's formulas) are found to be compatible with the contraction correction of the Theodorsen theory: the Goldstein theory, when rigidized, appears equivalent to the Theodorsen theory. In the Theodorsen theory, the required wake forces are seen to be so small that their neglect (by neglect of wake rigidity) is of conceptual significance only.

Nomenclature

A = cross-sectional area of one turn of helicoid wake at $z = \infty$ projected on Trefftz plane, πR_∞^2
B = number of blades
c_p = power coefficient, $\omega Q/(1/2)\rho V^3 \pi R_\infty^2$
c_s = thrust coefficient, $T/(1/2)\rho V^2 \pi R_\infty^2$
G_p = coefficient defined in Eq. (37)
G_s = coefficient defined in Eq. (36)
$K(x)$ = nondimensional blade circulation, $B\Gamma(x)/2\pi w \lambda_\infty R_\infty$
P = propeller power
Q = propeller torque
R_z = local radius of wake at z
R_0 = propeller radius, $R_0 = R_z$ for $z = 0$
R_∞ = asymptotic radius of wake, $z = \infty$
r = radial distance from propeller axis
S = suction force per unit length of wake edge
T = propeller thrust
V = propeller forward speed
v = disturbance velocity arising from axial speed w_z of helicoid turns, $-v_r$ = radial component, v_N = component normal to blade
w = rearward speed of helicoid wake turns relative to fluid at rest at $z = \infty$, $w \equiv w_\infty$
$\bar{w}$ = w/V
w_z = rearward speed of helicoid wake turns at section z relative to fluid at rest, barber pole analogy, pitch varies with z
x = r/R_z
z = axial distance downstream from propeller plane
$\Gamma(x)$ = blade circulation distribution, equals jump in velocity potential across helicoid surface at x
ΔR = wake contraction, $R_0 - R_\infty$
ε = axial loss factor of Theodorsen
η = ideal efficiency of propeller, c_s/c_p evaluated with blade profile drag neglected
κ = mass coefficient of Theodorsen
λ = propeller advance coefficient based on R_∞, $V/\omega R_\infty$
λ_z = local helicoid advance coefficient, $(V + w_z)/\omega R_\infty = V(1 + \bar{w}_z)/\omega R_\infty$: local R_z approximated as R_∞
λ_∞ = asymptotic helicoid advance coefficient, $(V + w_\infty)/\omega R_\infty$, designated λ_T in Refs. 5 and 6
ρ = fluid density
ϕ_z = local helix angle of wake edge, $\tan\phi_z = (V + w_z)/\omega R_z \approx \lambda_z$: Eq. (1)
ω = propeller angular velocity

Subscripts
e = effective value, a kind of weighted mean
m = maximum
N = normal component
prop = value ascribed to propeller
z = value at specified z
0 = value at $z = 0$
∞ = value at $z = \infty$

Introduction

THIS study introduces a paradigm shift into the prediction of the highest efficiency attainable by a propeller, neglecting profile drag, under specified operating conditions. Goldstein[1] and Theodorsen[2] model the wake of such an ideally loaded propeller in a special way. The freely trailing vortex sheet is supposed to have just the right vorticity distribution to be nondistorting in time: The helicoidal sheet from each blade moves backward, via the self-induced velocity field, as if rigid. It is argued here that these vortex sheets, the wake, must coexist with mathematically thin rigid massless surfaces. This physical rigidity (as distinct from induced rigid behavior) is an aspect overlooked in the original models.[1,2] The rigidity is required so that the wake may take up forces imposed by the fluid flow.

Received Nov. 11, 1997; revision received June 24, 1998; accepted for publication June 24, 1998.

*Professor Emeritus, Institute for Aerospace Studies, 4925 Dufferin Street; also Distinguished Research Associate, NASA Langley Research Center, Hampton, VA 23681-0001. Fellow AIAA.

Quoting from Ref. 3:

> The underlying scenario goes back to Betz,[4] implicitly for lightly loaded propellers . . . . . Goldstein[1] developed the analytic theory, leading to practical, accurate, performance prediction. Theodorsen[2,5,6] generalized this to apply, allowing for wake contraction, to heavily loaded propellers. He presented a rigorous proof that this rigid helicoid wake does indeed correspond to maximum efficiency for his flow model.

(For *rigid* here, read *nondeforming*, they did not postulate any stiffness or tensile strength for the wake.)

However, the forces on the rigid wake must be taken into account. In the Theodorsen model, revised to allow for rigidity, edge suction forces are tilted backward and circumferentially in the region of contraction. These are implicitly included in his predictions of propeller thrust and torque. The corrections are estimated herein. In the Goldstein model, again revised to allow for rigidity, the wake does not contract, but the streamlines do. The crossflow component, acting on the bound trailing vortices, generates aerodynamic lift; hence, thrust and torque components. These corrections are similarly estimated in this paper.

The following section develops and documents the arguments that the wake must be physically rigid.

Implied Wake Forces and Rigidity

Without wake forces the postulated rigid motion cannot occur, as pointed out by Schouten.[7,8] We quote Betz[9] for the analogous planar case:

> . . . this motion would only be possible for any length of time if the area of discontinuity [here the helicoid] actually were rigid. By flowing around the edges, laterally directed suction forces P occur, which only could be taken up by a rigid plate [helicoid]. These forces are absent when the area of discontinuity is other than rigid, as a result of which the suction P effects other motions: starting at the edges, it unrolls and gradually forms two distinct vortices.

Theodorsen's postulation of no roll-up is thus an imposition of rigidity: as a consequence, it indeed implies edge forces.

To elaborate on this, we observe that Theodorsen models the propeller and helicoidal wake system as being contained within a control surface. He obtains the thrust from an axial momentum balance for this surface, and the power from an energy balance. Clearly, the flow is the same outside the wake system whether or not the helicoids coexist with vanishingly thin rigid surfaces. Because the rigid surfaces sustain force from edge suction, this force will be accounted for in the momentum and energy balances. With this scenario, the axial momentum balance should yield the thrust of the composite structure: the propeller plus the wake extension. The thrust on the wake extension is thus a false contribution.

A direct calculation indicates the reality of the helicoid edge suction. In Ref. 10 a rotating rigid flat ribbon (a screw surface of infinite advance ratio) was modeled as the limiting form of a thin elliptic cylinder. The lateral component of the suction pressure on one half was integrated, extending from the top center to the bottom center. A finite force per unit length was obtained in the flat ribbon limit. This edge force was in agreement with that obtained in a more indirect fashion.

Goldstein[1] and Theodorsen[2] were fully aware that in reality the vortex sheets progressively deform: Goldstein remarked that they roll up into "as many helical vortices as there are blades". But both incorrectly attributed the deformation to instability. This implies that 1) a disturbance is required to start the deformation, and 2) lacking a disturbance there will be no deformation. The preceding quotation from Betz[9] corrects this interpretation: even with zero disturbance the vortex sheets must inevitably roll up. The key is that edge forces must be applied to prevent this.

The view herein is a variant from that put forward by Schouten[7,8]: "the half-infinite rigid helicoidal trailing vortex sheet system is unrealistic because it is not force-free. It could only survive as a bound system, capable of sustaining the edge forces." But the system is only unrealistic as a representation of free trailing vortex sheets. Indeed, one can model the propeller as having a rigid helicoidal extension.

The propeller plus rigid helicoidal extension is clearly an artifice: it may be compared with a real propeller behind which the initially helicoid wake rolls up[7,8] into helical tip vortices. The propellers are identical and operated at the same advance ratio. It is judged that, although the flow induced by the respective wakes is very different farther back, there is little difference at the propeller.[3,7,8] Accordingly, the propeller forces nearly match. Thus, for the combination, if the forces on the helicoidal extension are corrected for as in the preceding text, the results should closely approximate those on the real propeller. A detailed study in Ref. 3, including comparison with experiment (allowing then for friction drag), supported this conclusion.

Rigidized Theodorsen Model: Wake Edge Suction

The propeller–wake combination may be visualized as a rigid screw surface whose radius R contracts from the propeller radius R_0 to an asymptotic value R_∞ far back. It rotates with an angular velocity ω and advances axially through the fluid with speed V. Visualizing this screw surface somewhat like a rotating barber pole, the turns appear to move away from the propeller plane. But their inclination is such that they recede, not with speed V, but with speed $V + w_z$. Thus, the turns are pushing backward through the surrounding fluid with a velocity w_z; owing to decreasing pitch, this varies with distance z behind the propeller from w_∞ far back ($z = \infty$) to about 1/2 w_∞ at $z = 0$.[2] The backward motion, with normal component v_N, gives rise to a crossflow around the inclined edges (Fig. 1). It is this high-speed crossflow, singular at the edge, that causes the suction.

The relevant geometry is as follows. Approximating the local R by R_∞, the edge helix angle at axial distance z is given by

$$\tan \phi_z = (V + w_z)/\omega R_\infty \equiv \lambda_z \tag{1}$$

The local edge normal velocity is

$$v_N = w_z \cos \phi_z \tag{2}$$

and the normal distance between turns is

$$L_N = L \cos \phi_z \tag{3}$$

in terms of the axial separation L.

In a given helicoid, the circulation $\Gamma(r)$ at a very small distance $R - r$ from the edge varies like $\sqrt{R - r}$. This is associated with a suction force that in two-dimensional flow takes the form

$$S = \lim_{r \to R} (\pi/8)\rho[\Gamma(r)/\sqrt{R - r}]^2 \tag{4}$$

per unit length of edge. Equation (4) is inferred from an equivalent relation of Garrick.[12] It is considered to apply locally far back ($z \to \infty$) to a good approximation.

A normalized version of $\Gamma(r/R)$ is $K(r/R)$, defined by

$$K(x) = \omega B\Gamma(x)/2\pi w_\infty(V + w_\infty) = B\Gamma(x)/2\pi w_\infty \lambda_\infty R_\infty, \quad x = r/R \tag{5}$$

so that in terms of K and the definition of λ_z in Eq. (1)

$$S_z = \rho w_z^2 R_\infty(\pi^3/4B^2)\lambda_\infty^2[K(x)/\sqrt{1 - x}]^2 \tag{6}$$

This can be evaluated from Theodorsen's[2] or Foster's[6] plots of $K(x, B)$.

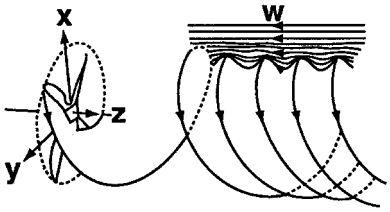

Fig. 1 Flow across edges of helicoid wake because of its backward velocity w relative to the fluid. (Very schematic: obscures effect of edge inclination.) Adapted from Fig. 3 of Ref. 11.

At smaller values of z, the progressive reduction of w_z, alluded to earlier, diminishes the suction. We are guided by a relation discussed later in some detail for the flow past a stack of flat plates: the edge suction scales as the product of edge normal velocity squared and normal separation. In the helicoid context, we interpret these as edge normal velocity v_N and normal separation L_N. Applying this scaling to generalize Eq. (1) from $z \to \infty$ to arbitrary z requires a scaling factor of $(v_N^2 L_N)_z/(v_N^2 L_N)_\infty$. The result is, using Eqs. (1–3)

$$S_z = \rho w_z^2 R_\infty \frac{\pi^3(1+\lambda_\infty^2)^{3/2}}{4B^2(1+\lambda_z^2)^{3/2}} \lambda_\infty^2 \left(\frac{K(x)}{\sqrt{1-x}}\right)^2 \tag{7}$$

The suction force $d\boldsymbol{F}$ on an element ds of the edge lies along a unit normal $\boldsymbol{n}$ in the tangent plane of the edge

$$d\boldsymbol{F}_z = S_z \boldsymbol{n}\, ds = S_z \boldsymbol{n} \frac{ds}{dR} dR \tag{8}$$

noting that R varies with z. The normal $\boldsymbol{n}$ and ds/dR are evaluated from the geometry of the helicoid. The backward and circumferential tilts of $\boldsymbol{n}$ and, hence, of $d\boldsymbol{F}_z$, (dR being negative in the contraction) give rise to negative thrust and positive torque contributions.

The backward tilt of the suction increment $d\boldsymbol{F}_z$ is shown schematically in Fig. 2. The rigid wake portrayed here is almost plane: it resembles a slightly twisted ribbon. The scenario applies to a propeller operating at very high advance ratio: a limiting case. At moderate advance ratio (Fig. 1) the wake exhibits a substantial helicoidal twist: the circumferential tilt of $d\boldsymbol{F}_z$ then becomes significant as well.

The tangent of the local wake edge helix angle ϕ_z is the advance ratio λ_z defined in Eq. (1). Thus, λ_z figures in evaluating the tangent plane of the edge and, hence, the edge normal $\boldsymbol{n}$ of Eq. (8). Omitting details of the geometric analysis, the incremental thrust and torque provided by the wake are found to be

$$dT = \frac{BS_z\lambda_z}{\sqrt{1+\lambda_z^2}} dR \tag{9}$$

$$dQ = -\frac{BS_z R_z}{\sqrt{1+\lambda_z^2}} dR \tag{10}$$

The corrected propeller thrust is the predicted thrust according to Theodorsen[2] minus the thrust dT on the wake. A similar remark applies for the corrected torque.

In what follows, as well as in accurate implementation of the Theodorsen theory, the total wake contraction $\Delta R = R_0 - R_\infty$ will appear as a parameter. Theodorsen evaluated ΔR by equating two versions of the thrust. One was the thrust evaluated directly from the predicted lift on the propeller blades of radius R_0; the other was the thrust inferred from the momentum balance involving the wake of asymptotic radius R_∞. Theodorsen devotes a chapter to the estimation of ΔR for $w/V \ll 1$; the curves of his Fig. 29 are approximately collapsed in an empirical equation given in Ref. 5. But a much more

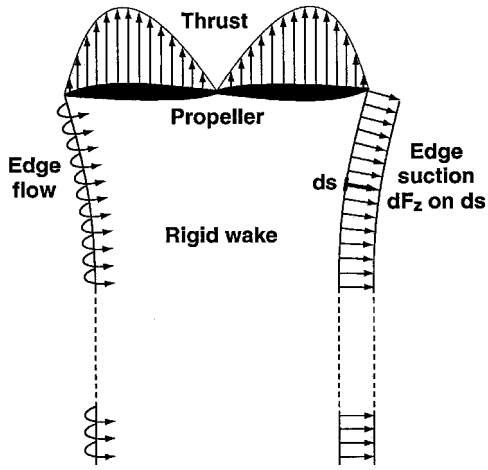

Fig. 2 Schematic portrayal of two-blade propeller operating at very high advance ratio: wake resembles a slightly twisted ribbon. LHS shows edge flow and RHS shows resulting edge suction force.

accurate evaluation for values of w/V up to 2 is available in the charts of Ref. 6: these were used in evaluating ΔR for the tables appearing herein.

Numerous estimates have shown that, upon integration over the contraction, which is small, these corrections rarely exceed 1%, thus, efforts toward high precision in their determination seems unwarranted. The contraction ratio $\Delta R/R_\infty$, although listed later to three significant figures, is really accurate to no more than two. Moreover, the specified variation of the edge suction scaling factor with w_z in the contracting region is merely an assumption. Thus, on integrating Eqs. (9) and (10), it seems justified to treat the integrands as constant: each would be evaluated at some fixed value of z estimated to yield the same integral. In an example calculation for large wake velocity ($w_\infty/V = 1.0$), this corresponded to an effective value of w_z given by $w_z = 0.80 w_\infty \equiv w_e$. (In what follows, w_∞ is designated simply w.)

With the integrand fixed at the value corresponding to w_e, Eqs. (9) and (10) may be integrated, as R contracts by a total amount $\Delta R = (R_0 - R_\infty)$, to give

$$\Delta T = -(BS_e\lambda_e/\sqrt{1+\lambda_e^2})\Delta R \tag{11}$$

$$\Delta Q = (BS_e R_\infty/\sqrt{1+\lambda_e^2})\Delta R \tag{12}$$

The sign reversal reflects ΔR and dR having opposite signs; further, R_e has been approximated as R_∞ in the factor, the difference being very small. Corresponding nondimensional thrust and power coefficients may be defined as

$$\Delta c_s = \Delta T/(1/2)\rho V^2 \pi R_\infty^2 \tag{13}$$

$$\Delta c_p = \omega \Delta Q/(1/2)\rho V^3 \pi R_\infty^2 \tag{14}$$

On inserting Eqs. (7), (11), and (12), these are evaluated as

$$\Delta c_s = -\frac{\pi^2}{2B} \bar{w}_e^2 \frac{(1+\lambda_\infty^2)^{3/2}}{(1+\lambda_e^2)^2} \lambda_e \lambda_\infty^2 \left[\frac{K(x)}{\sqrt{1-x}}\right]^2 \frac{\Delta R}{R_\infty} \tag{15}$$

$$\Delta c_p = \frac{\pi^2}{2B} \bar{w}_e^2 \frac{(1+\lambda_\infty^2)^{3/2}}{(1+\lambda_e^2)^2} \frac{\lambda_\infty^2}{\lambda} \left[\frac{K(x)}{\sqrt{1-x}}\right]^2 \frac{\Delta R}{R_\infty} \tag{16}$$

Sample calculations show that the largest wake force contributions occur at small propeller advance ratio λ and large relative wake velocity $\bar{w} \equiv w/V$. We first show calculations for $\lambda = 0.1$, and for two and four propeller blades ($B = 2,4$). These are cases for which curves of $K(x)$ are available (Theodorsen,[2] $B = 2,4$; Foster,[6] $B = 2$). The parameter $\bar{w}$ ranges from

Table 1 Propeller edge force corrections

$\bar{w}$	$\bar{w}_e$	λ_e	$\lambda_\infty(K\sqrt{1-x})_{\mu}$	$\Delta R/R_\infty$	$100\Delta c_s$	$100\Delta c_p$	c_s	c_p	$c_s/c_p = \eta$	$100\Delta\eta$, %
				$\lambda = 0.1, B = 2$						
0.2	0.160	0.116	0.286	0.0325	−0.0019	0.167	0.398	0.440	0.905	0.35
0.4	0.320	0.132	0.320	0.0493	−0.0167	1.269	0.896	1.090	0.822	0.98
1.0	0.800	0.180	0.375	0.0650	−0.2585	14.364	2.748	4.252	0.646	2.32
				$\lambda = 0.1, B = 4$						
0.2	0.150	0.116	0.552	0.357	−0.0040	0.342	0.439	0.486	0.940	0.65
0.4	0.320	0.132	0.549	0.0562	−0.0281	2.128	1.028	1.253	0.820	1.44
1.0	0.800	0.180	0.536	0.0832	−0.3380	18.78	3.401	5.320	0.639	2.40

Table 2 Propeller edge force corrections[a]

B	$\bar{w}$	$\bar{w}_e$	λ_e	(b_p)	$\Delta R/R_\infty$	$100\Delta c_s$	$100\Delta c_p$	c_s	c_p	$c_s/c_p = \eta$	$100\Delta\eta$, %
2	1.0	0.800	0.180	0.0389	0.0650	−0.253	14.05	2.748	4.252	0.646	2.27
4	1.0	0.800	0.180	0.0389	0.0858	−0.334	18.55	3.401	5.320	0.639	2.37
8	1.0	0.800	0.180	0.0389	0.0958	−0.373	20.71	3.423	5.353	0.639	2.65
12	1.0	0.800	0.180	0.0389	0.1000	−0.389	21.62	3.663	5.772	0.635	2.54
∞	1.0	0.800	0.180	0.0389	0.1064	−0.414	23.00	4.165	6.590	0.632	2.35

[a]For large numbers of blades via the Prandtl approximation,[13] $\lambda = 0.1$.

0.2 to 1.0. Because $\bar{w}$ (related to the heaviness of loading) doesn't exceed 0.5 for propeller scenarios that we have encountered,[3] the choice $\bar{w} = 1.0$ represents an extreme upper limit.

In Table 1, c_s and c_p refer to values for the propeller-wake combination calculated from Theodorsen's formulas[2]; they result from momentum and energy balances, respectively, for the composite contained within a control surface:

$$c_s = 2\kappa\bar{w}[1 + \bar{w}(1/2 + \varepsilon/\kappa)] \tag{17}$$

$$c_p = 2\kappa\bar{w}(1 + \bar{w})(1 + \bar{w}\varepsilon/\kappa) \tag{18}$$

They are evaluated using plots of κ and ε/κ vs $\lambda_T = \lambda(1 + \bar{w})$ from Ref. 6, with λ_T therein replaced by λ_e; as noted, $\bar{w}_e$ will be taken as $0.80\bar{w}$ in λ_e. The respective parts attributed to the propeller alone are $(c_s)_{\text{prop}} = c_s - \Delta c_s$ and $(c_p)_{\text{prop}} = c_p - \Delta c_p$. Thus, the increment to be added to the Theodorsen efficiency, $\eta = c_s/c_p$, to correct for edge forces on the wake is

$$\Delta\eta = \frac{(c_s)_{\text{prop}}}{(c_p)_{\text{prop}}} - \frac{c_s}{c_p} = \frac{c_s - \Delta c_s}{c_p - \Delta c_p} - \frac{c_s}{c_p} \tag{19}$$

Three to four decimal places are retained in Table 1, after rounding down, although the accuracy is less. The final values of $\Delta\eta$ are most likely accurate to no more than two figures.

Prandtl Aproximation: Wake Edge Suction

For blade numbers B greater than four (single rotation), published curves of $K(x)$ with adequate detail near $x = 1$ do not appear to be available. Thus, we turn to an approximate flow model from Prandtl,[13] whose predictions of edge force should approach the correct value for large B. In this model the interleaved helicoids of Theodorsen's model[2] are replaced locally by a tangent set of of semi-infinite flat plates of the same inclination and spacing. The suction force S on the edges of these equivalent plates is[8]

$$S_z = \rho v_N^2 L_N/2 \tag{20}$$

per unit length. Here, v_N is the component normal to the plates of the local backward velocity w_z of the helicoid, and L_N is their normal separation. It follows from the geometry [Eqs. (1–3)] that

$$S_z = \frac{\pi}{B}\rho\bar{w}_z^2 R_\infty \frac{\lambda_z}{(1 + \lambda_z^2)^{3/2}} \tag{21}$$

This leads, multiplying by the number of helicoids B, and fixing λ_z at the effective average value λ_e, to

$$\Delta c_s = -\left[2\bar{w}_e^2 \frac{\lambda_e^2}{(1 + \lambda_e^2)^2}\right]\frac{\Delta R}{R_\infty} \equiv -(b_p)\frac{\Delta R}{R_\infty} \tag{22}$$

$$\Delta c_p = -\Delta c_s/\lambda\lambda_e \tag{23}$$

In Table 2, values of Δc_s and Δc_p are evaluated for numbers of blades B ranging from 2 to ∞. The corresponding changes in propeller efficiency are given in the last column. These calculations are limited to the extreme value of $\bar{w} = 1$: much smaller values would be expected for propellers in practice.[3] The objective was to display the variation of $\Delta\eta$ with number of blades B in a worst-case scenario. The variation is seen to be minimal.

Rigidized Goldstein Model: Wake Normal Force

Goldstein's[1] vortex theory of screw propellers models the wake as B interleaved helicoids of constant radius R_0. Like Theodorsen's[2] wake, it is supposed to be a system of freely trailing vortex sheets, but it differs in not allowing for contraction. Here, again, it is a requirement that each sheet coincide with a mathematically thin rigid surface capable of resisting force; otherwise, the postulated flow is not possible. With no contraction, the suction force on the edges of the surfaces is radial everywhere. Because this edge force contributes to neither thrust nor torque, it may ignored.

Goldstein largely limited his analysis to providing the optimum $\Gamma(r/R)$, or equivalently $K(x)$, for the propeller. But consider Theodorsen's predictive equations (17) and (18) that result from momentum and energy balances for a control surface: these should apply as well to Goldstein's noncontracting wake of radius R_0; a prerequisite is that we allow for any wake forces. We refer to this application of Theodorsen's formulas as the *rigidized* Goldstein theory.

Although the edge forces in this model are purely radial, the rigid wake surfaces may experience normal forces: these can contribute to thrust and torque. They arise from the radial inflow v_r that causes Theodorsen's contraction. The trailing vor-

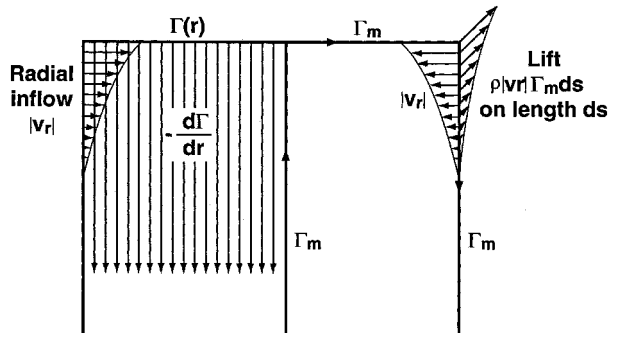

Fig. 3 Scenario of Fig. 2. LHS shows actual distributed vorticity $-d\Gamma/dr$. RHS shows replacement by horseshoe vortex of circulation Γ_m. Aerodynamic lift because of radial inflow v_r is shown schematically.

tices of strength $-d\Gamma/dr$ are essentially bound in the rigid surface: being normal to v_r, they will experience a normal force $\rho(-d\Gamma/dr)v_r$ per unit area as aerodynamic lift. (The trailing vortices in Theodorsen's[2] scenario experience no normal force; they follow the curved streamlines that include v_r.)

Determination of the radial variation of v_r at a given z would offer considerable difficulty: we sidestep this by evaluating an upper limit to the normal force. We replace the trailing sheet $-d\Gamma/dr$ by its integral from the peak, Γ_m, of the blade span loading to the tip where $\Gamma = 0$. This is treated as a line vortex of circulation Γ_m running along the outer edge of the trailing sheet. Because $v(r)$ maximizes at $r = R$, this replacement ensures an upper limit to the integrated normal force. Figure 3 shows schematically the distributed wake vorticity on the left-hand side (LHS) and the replacement horseshoe vortex on the right-hand side (RHS); reference is to a wake at very high advance ratio, hence, there is very little twist, as in Fig. 2.

The normal force on a length ds of the B wakes is thus

$$dN = B\rho\Gamma_m v_r(R, z)\, ds = B\rho\Gamma_m v_r \frac{dz}{\sin\phi_z} \tag{24}$$

with thrust and torque components

$$dT = dN\cos\phi_z = B\rho\Gamma_m v_r \cot\phi_z\, dz \tag{25}$$

$$dQ = R\, dN \sin\phi_z = B\rho\Gamma_m v_r\, dz \tag{26}$$

Here, ϕ_z is the local helix angle at axial distance z, given by Eq. (1). To evaluate v_r, we revert, for this purpose only, to Theodorsen's model in which the helicoids contract from R_0 to an asymptotic radius R_∞: thus, v_r (taken positive inward) is taken as local axial velocity times $(-dR/dz)$. This gives

$$v_r\, dz = -(V + w_z)\, dR = -V(1 + \bar{w}_z)\, dR \tag{27}$$

and from Eq. (5)

$$\Gamma_m = 2\pi K_m \bar{w}_\infty V^2(1 + \bar{w}_\infty)/\omega B \tag{28}$$

Then Eqs. (25) and (26) respectively become, using the definition $\bar{w} \equiv \bar{w}_\infty$

$$dT = -2\pi\rho K_m \bar{w} V^2(1 + \bar{w})R_\infty\, dR \tag{29}$$

$$dQ = -2\pi\rho K_m \bar{w} V^3 \frac{(1 + \bar{w})^2}{\omega R_\infty} R_z^2\, dR \tag{30}$$

Integrating along the contraction replaces dR by $(R_\infty - R_0) = -\Delta R$, dT by ΔT_G, and dQ by ΔQ_G (the subscript G referring to the Goldstein model). For an estimation of K_m, we take $K(x)$, as a rough approximation, to be parabolic: then it is easily shown that

$$K_m = \frac{3}{2}\int_0^1 2xK(x)\, dx = \frac{3}{2}\kappa \tag{31}$$

according to Theodorsen's definition of the parameter k. With these three replacements

$$\Delta T_G = 3\pi\rho V^2 R_z^2 \kappa\bar{w}(1 + \bar{w})\Delta R/R_\infty \tag{32}$$

$$\Delta P_G = \omega\Delta Q = 3\pi\rho V^3 R_\infty^2 \kappa\bar{w}(1 + \bar{w})^2\Delta R/R_\infty \tag{33}$$

These are the contributions arising from aerodynamic lift on the rigidized wake: they are to be subtracted, respectively, from the thrust T_G and power P_G determined via the Goldstein noncontracting wake model. For comparison, the cited momentum and energy balances show that the predicted T_G and P_G are scaled up from those of Theodorsen in the ratio of their respective wake areas. That is, the values based on the Goldstein wake are too large in the ratio R_0^2/R_∞^2. (Correction of this is a major feature of Theodorsen's model.) Thus, if we nondimensionalize by R_0 instead of R_∞ (see the Nomenclature), Eqs. (17) and (18) will carry over to the Goldstein model. On this understanding

$$T_G = c_s(1/2)\rho V^2\pi R_0^2 = 2\kappa\bar{w}[1 + \bar{w}(1/2 + \varepsilon/\kappa)](1/2)\rho V^2\pi R_0^2 \tag{34}$$

$$P_G = c_p(1/2)\rho V^3\pi R_0^2 = 2\kappa\bar{w}(1 + \bar{w})(1 + \bar{w}\varepsilon/\kappa)(1/2)\rho V^3\pi R_0^2 \tag{35}$$

The ratios of the spurious wake contributions to the respective thrust and power are then

$$\frac{\Delta T_G}{T_G} = \frac{3(1 + \bar{w})}{1 + \bar{w}(1/2 + \varepsilon/\kappa)}\frac{R_\infty^2}{R_0^2}\frac{\Delta R}{R_\infty} \equiv G_s\frac{R_\infty^2}{R_0^2}\frac{\Delta R}{R_\infty} \approx G_s\frac{\Delta R}{R_\infty} \tag{36}$$

$$\frac{\Delta P_G}{P_G} = \frac{3(1 + \bar{w})}{1 + \bar{w}\varepsilon/\kappa}\frac{R_\infty^2}{R_0^2}\frac{\Delta R}{R_\infty} \equiv G_p\frac{R_\infty^2}{R_0^2}\frac{\Delta R}{R_\infty} \approx G_p\frac{\Delta R}{R_\infty} \tag{37}$$

where terms of order $(\Delta R/R_\infty)^2$ are neglected (see an expansion of R_∞^2/R_0^2 in the following text).

As noted, the differing radii of the wakes accounts for the following relations connecting the Theodorsen thrust T_T and power P_T and the corresponding Goldstein thrust T_G and P_G:

$$T_T = \frac{R_\infty^2}{R_0^2}T_G = \frac{T_G}{(1 - \Delta R/R_\infty)^2} \approx T_G\left(1 - 2\frac{\Delta R}{R_\infty}\right) \tag{38}$$

$$P_T = \frac{R_\infty^2}{R_0^2}P_G = \frac{P_G}{(1 - \Delta R/R_\infty)^2} \approx P_G\left(1 - 2\frac{\Delta R}{R_\infty}\right) \tag{39}$$

Restated in the format of Eqs. (36) and (37)

$$\Delta T_T/T_G = 2(\Delta R/R_\infty) \tag{40}$$

$$\Delta P_T/P_G = 2(\Delta R/R_\infty) \tag{41}$$

Our rigidized Goldstein theory predictions, Eqs. (36) and (37), would agree with the corresponding Theodorsen predictions, Eqs. (40) and (41), if G_s and G_p were both equal to 2. We find that for $\bar{w} = 0$, $G_s = 3$, and $G_p = 3$; and for $\bar{w} = 1.0$, $\lambda = 0.1$, and $B = 4$, $G_s = 2.6$, and $G_p = 3.3$. Recalling that G_s and G_p, owing to the types of approximation, are upper bounds, their excess over 2 is quite reasonable. Thus, the inference of equivalence of the rigidized Goldstein theory with the Theodorsen theory appears quite credible. (This imprecise

comparison justifiably leaves out the much smaller edge forces that Theodorsen omits from his theory.)

Conclusions

1) The postulated helicoid wake in both the Theodorsen and Goldstein theories must be physically rigid: it must be capable of withstanding forces imposed by the flow to persist undeformed. The forces may be tensile (from edge suction) or normal (from aerodynamic lift).

2) The nonrigid wake will inexorably roll up, even in the absence of any initial disturbance. This conflicts with the notion[1,2] that roll-up is merely the manifestation of wake instability.

3) In the rigidized Theodorsen theory, wake edge forces in the region of contraction make only very small changes to the otherwise predicted thrust and torque. Being of opposite sign, they change the efficiency as well. In the tabulated calculations the change, a gain, is in most cases under 1%; but it can reach over 2% for very heavy loading.

4) On the Goldstein model, the wake radius remains constant: radial inflow replaces Theodorsen's contraction. The rigidization required by 1 then allows the wake to develop aerodynamic lift locally, the trailing vortices being at right angles to the radial inflow. Upper limits of the corresponding increments of thrust and torque have been evaluated. These were found compatible with those arising from the contraction in Theodorsen theory. Thus, the rigidized Goldstein theory appears essentially equivalent to the Theodorsen theory.

5) In the Theodorsen theory, the required wake forces are seen to be so small that their neglect (by neglect of wake rigidity) is of conceptual significance only. As a practical matter, the labor of incorporating wake force corrections is not warranted.

Acknowledgments

Support at the University of Toronto was aided by a Grant from the Natural Sciences and Engineering Research Council of Canada and at NASA Langley Research Center by tenure as a Distinguished Research Associate.

References

[1]Goldstein, S., "On the Vortex Theory of Screw Propellers," *Proceedings of the Royal Society of London*, Series A, Vol. 123, No. 792, 1929, pp. 440–465.

[2]Theodorsen, T., *Theory of Propellers*, McGraw–Hill, New York, 1948.

[3]Ribner, H. S., "Neglect of Wake Rollup in Theodorsen's Theory of Propellers," *Journal of Aircraft*, Vol. 34, No. 6, 1997, pp. 814–816.

[4]Betz, A., "Screwpropeller with Least Energy Loss," Göttinger Nachrichten, 1919, pp. 192–213 (in German); also reprinted in *Vier Abhandlungen zur Hydrodynamik und Aeodynamik*, Göttingen, Germany, 1927, pp. 68–92.

[5]Ribner, H. S., and Foster, S. P., "Ideal Efficiency of Propellers: Theodorsen Revisited," *Journal of Aircraft*, Vol. 27, No. 9, 1990, pp. 810–819.

[6]Foster, S. P., "Ideal Efficiency of Propellers Based on Theodorsen's Theory: A Review and Computer Study, with Extended Plus Simplified Charts," Univ. of Toronto, Inst. for Aerospace Studies, UTIAS TN 271, Downsview, ON, Canada, Feb. 1991.

[7]Schouten, G., "Static Pressure in the Slipstream of a Propeller," *Journal of Aircraft*, Vol. 19, No. 3, 1982, pp. 251, 252.

[8]Schouten, G., "Theodorsen's Ideal Propeller Performance with Ambient Pressure in the Slipstream," *Journal of Aircraft*, Vol. 30, No. 3, 1993, pp. 417–419.

[9]Betz, A., "Behavior of Vortex Systems," *Zeitschrift fuer Angewandte Mathematik und Mechanik*, Vol. 12, No. 3, 1932, pp. 164–174; also translated as NACA TM 713, 1933.

[10]Ribner, H. S., "A Transonic Propeller of Triangular Plan Form," NACA TN 1303, May 1947.

[11]Lock, C. N. H., "An Application of Prandtl Theory to an Airscrew," British Aeronautical Research Council, R&M 1521, Aug. 1932.

[12]Garrick, I. E., "Propulsion of a Flapping and Oscillating Airfoil," NACA 567, 1936, pp. 1–7.

[13]Prandtl, L., "Tragflachentheorie I & II," *Nachrichter der Koninglichen Gesellschaft der Wissenschaften zu Gottingen, Mathematisch-Physische Klasse*, 1918, p. 451; 1919, p. 107; also NACA TR 116, 1921.